ELSEVIER

Journal of Alloys and Compounds 323–324 (2001) 558–561

Journal of ALLOYS AND COMPOUNDS

www.elsevier.com/locate/jallcom

High-resolution and energy-filtered transmission electron microscopy of $YBa_2Cu_3O_{7-x}/PrBa_2Cu_3O_7$ superlattices

M. Varela[a], C. Ballesteros[a,*], W. Grogger[b], K.M. Krishnan[b], D. Arias[c,1], Z. Sefrioui[c], C. León[c], J. Santamaría[c]

[a]Dpto. Fisica, Universidad Carlos III de Madrid, Avda de la Universidad 30, 28911 Leganés, Madrid, Spain
[b]Materials Sciences Division, 72-222, Lawrence Berkeley National Laboratory, University of California, Berkeley, CA 94720, USA
[c]Dpto. Fisica Aplicada III, Universidad Complutense, Ciudad Universitaria, 28040 Madrid, Spain

Abstract

Structural disorder induced by epitaxial strain relaxation in *c*-axis oriented $[YBa_2Cu_3O_{7-x\ n\ \mathrm{u.c}}/PrBa_2Cu_3O_{7\ 5\ \mathrm{u.c.}}]$ superlattices on (100) $SrTiO_3$ substrates has been analyzed by high-resolution and energy-filtered transmission electron microscopy. Epitaxial strain shows up in ultrathin YBCO layers with thickness below 4 unit cells. Strain relaxation takes place when layer thickness increases above this value. Microscopy observations for epitaxially strained superlattices show a good morphology of the layers, with sharp and flat interfaces. However, in relaxed samples rougher interfaces are observed, together with microdomains showing the *c*-axis parallel to the substrate plane which preserve the superlattice compositional profile. Such microdomains of *c*-parallel growth provide a path for reduced lattice mismatch, conforming a very efficient mechanism for strain relaxation.

Keywords: A. high-Tc superconductors; A. thin films; C. scanning and transmission electron microscopy

Introduction

The complex structure of high critical temperature superconductors (HTCS) makes the physical properties of ultra-thin HTCS epitaxial films strongly dependent on layer thickness and epitaxial strain [1]. In the particular case of a superlattice structure, lattice mismatch between the materials involved may seriously affect the structure and morphology of ultrathin layers of the constituent materials. In this frame, considerable attention has been paid to the study of the intracell structure under epitaxial strain, as a way to modify the superconducting properties [2,3]. The strain energy is elastically accommodated in the lattice and increases with layer thickness. There is a critical thickness for strain relaxation, which is accompanied by significant changes in the microstructure. The intracell and intralayer features must be analyzed, because not only the intracell distances but also the structural disorder eventually present within superlattice layers (layer discontinuities, grain boundaries, dislocations, etc.) may seriously affect the superconducting behavior [4].

In a previous work, $YBa_2Cu_3O_{7-x}$ (YBCO)/$PrBa_2Cu_3O_7$ (PBCO) superlattices have been analyzed by X-ray diffraction (XRD) [3]. For YBCO layer thickness below 4 unit cells, XRD refinement indicates no interfacial roughness, denoting sharp and flat interfaces; but when YBCO layer thickness grows a gradual increase of the interfacial roughness is observed [4]. XRD provides structural information averaged over long lateral scales but the local microstructure of the defects introduced by strain relaxation remains unexplored. In this work we present a study of the nature of such defects in YBCO/PBCO superlattices by high-resolution and energy-filtered transmission electron microscopy (HREM and EFTEM, respectively). These are powerful techniques to obtain structural information in the real space about the structure and distribution of defects. While HREM gives structural information at atomic scale, energy-filtered imaging provides a tool to study the spatial distribution of an element on the nanometer scale by selecting an energy loss corresponding to a characteristic inner-shell excitation [5,6]. Thus, it can be used to acquire elemental distribution images at high lateral resolution, providing conclusive support for the superlattice chemical composition.

*Corresponding author.
[1]On leave from Universidad del Quindio, Armenia, Colombia.

0925-8388/01/$ – see front matter
PII: S0925-8388(01)01143-4

Experimental

[$YBCO_{n\ u.c.}$/$PBCO_{5\ u.c.}$] superlattices where grown on $SrTiO_3$ substrates, by high pressure (3.6 mbar pure oxygen) sputtering system, under experimental conditions described in Ref [3]. YBCO layer thickness was changed from $n=1$ to $n=12$ unit cells, while PBCO layers where held constant in 5 unit cells (60 Å). Films were grown to the same total thickness of 1000 Å. Cross-sectional samples for TEM were prepared by conventional mechanical grinding, dimpling and argon ion milling with an acceleration voltage of 5 kV and an incidence angle of 8°. Analytical electron microscopy investigations were carried out using a Jeol 4000EX and a Philips CM200-FEG TEM equipped with a Gatan Imaging Filter, capable of obtaining both electron energy-loss spectra and energy-filtered images in real time at high spatial resolution.

Results and discussion

The structure of this kind of samples has been extensively studied by HREM [7]. However, we performed some HREM observations in order to directly observe the structural effects associated with epitaxial strain relaxation. Cross-sectional images with the *c*-axis of the film perpendicular to the electron beam confirmed that the strained superlattices have a pure *c*-axis orientation, [001], with the *c*-axis perpendicular to the substrate plane. The good morphology and lateral uniformity of the layers is observed in Fig. 1a,b for a typical [$YBCO_1$/$PBCO_5$] sample. A cross-section image is a projection of the structure over the specimen thickness (around 25 nm) and no differences can be observed between the two possible [001] orientations, with the *a*-axis parallel or perpendicular to the plane of the image (see Fig. 1b). The most widely observed type of defects in all kinds of samples were antiphase boundaries with a displacement of $c/3$ along the [001] direction, as a result of substrate steps one unit cell high ($c/3$).

Unfortunately, HREM images do not show compositional contrast between YBCO and PBCO layers, due to their similar crystal structure. Meanwhile, energy-filtered imaging allows clearly to resolve interface features. For imaging of these superlattices we used the low energy Y–$M_{4,5}$ and Pr–$N_{4,5}$ ionization edges applying the two window technique (jump ratio images) [5,6]. In terms of signal these low-loss edges are highly superior to their higher-loss counterparts. Since we were not interested in quantitative results we acquired jump-ratio images better than elemental maps. Due to the vicinity of plasmons as well as due to the close distance of the two edges, it is not possible to acquire elemental maps in this energy range without sophisticated procedures for background extrapolation and edge fitting/deconvolution. Both pre-edge and post-edge images were acquired within short acquisition times to reduce specimen drift and/or irradiation damage, and the ratio between them was calculated to show the spatial distribution of both Y and Pr ions. Fig. 2 shows a set of bright field and energy-filtered images from a [$YBCO_3$/$PBCO_5$] sample, showing complementary chemical information. Some amount of elastic contrast is transferred to the images, and hence, lattice planes can be observed. In this epitaxially strained superlattice, perfectly smooth layers of uniform thickness are seen, in good agreement with the absence of noticeable roughness denoted by X-ray fitting.

On the other hand, the study of relaxed samples showed inhomogeneous distributions of microdomains with the *c*-axis parallel to the substrate plane, i.e., perpendicular to

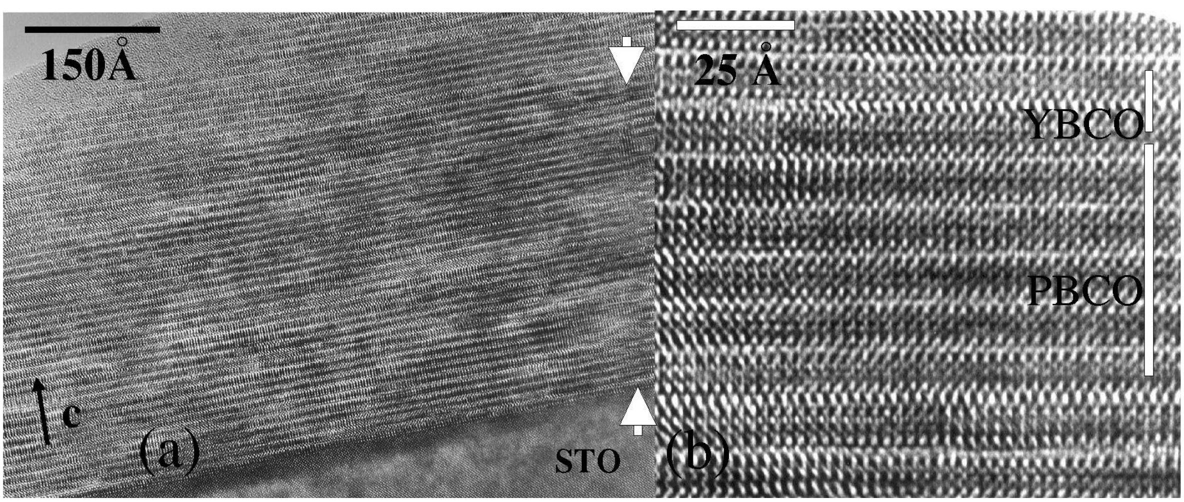

Fig. 1. (a) Low magnification image of a [$YBCO_1$/$PBCO_5$]$_{1000\ Å}$ sample, with the *c*-axis perpendicular to the electron beam. (b) HREM image from the same sample. Observe an antiphase boundary emerging from a substrate step (marked with arrows).

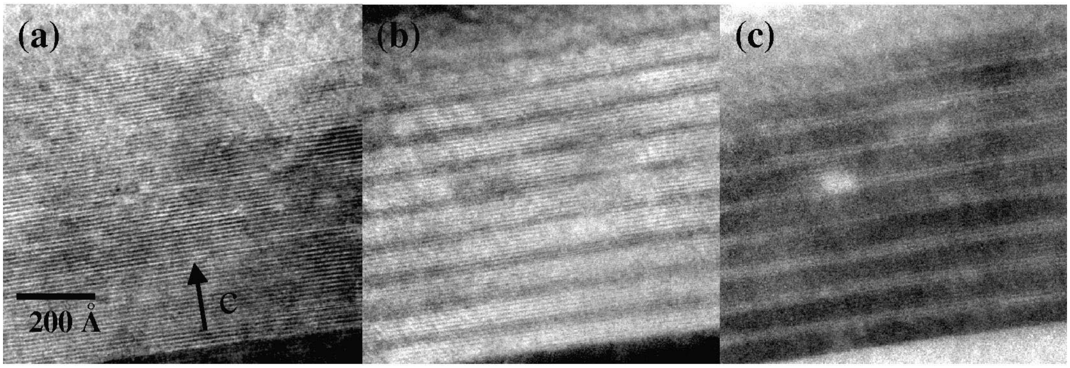

Fig. 2. (a) Bright-field image from a $[YBCO_3/PBCO_5]_{1000\ Å}$ sample. Such imaging conditions hardly show any compositional contrast between YBCO and PBCO. (b) Pr map and (c) Y map, showing sharp interfaces.

the growth direction, an example is shown in Fig. 3a. This is a different type of defect, commonly found by TEM, that could not be detected by XRD. Film growth under this orientation has been obtained at substantially lower substrate temperatures as 600–750°C [8,9], but is unexpected at so high growth temperatures as 900°C. Such microdomains were only found in relaxed superlattices, not showing up in the strained ones, and their spatial distribution or their size is quite inhomogeneous. They can emerge from the substrate plane or from some intermediate stage of the film growth, even close to the sample surface. The chance of such microdomains being extrinsic factors to the superlattice growth must be ruled out. The EFTEM characterization of *c*-axis in plane microdomains, shown in Fig. 3b, confirms that these microtwins do preserve the superlattice compositional contrast. Additionally, they show a modulation wavelength of 145 Å, the same one than the rest of the superlattice and in good agreement with the value of 150 Å extracted from XRD fitting. In fact, *a*-axis growth provides a path for a reduction in lattice mismatch in the wide distributions of these *a*-axis oriented microtwins. While for *c*-axis orientation the in-plane lattice parameters show a difference of $\epsilon_a = 0.007$ and $\epsilon_b = 0.011$, for parallel *c*-axis orientation $\epsilon_c = 0.005$, which leads to a reduction of interface mismatch (see Fig. 3). Thus, *c*-parallel oriented microdomains might appear as an in-

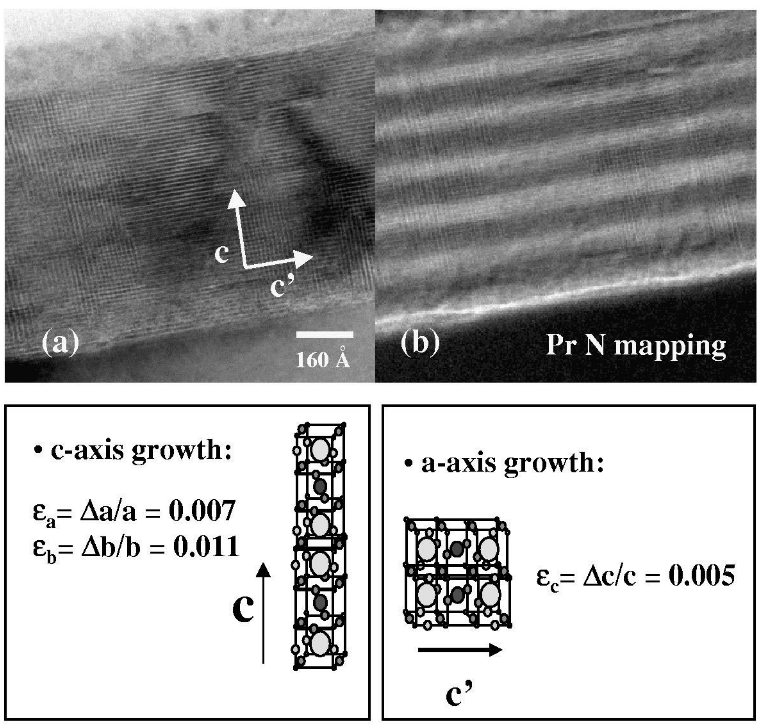

Fig. 3. (a) Images from a $[YBCO_8/PBCO_5]_{1000\ Å}$ relaxed sample, showing an inhomogeneous distribution of *a*-axis oriented microdomains. (b) Pr map of the same zone. These microdomains preserve the superlattice compositional profile. (c) *a*-Axis oriented growth provides a path for lattice mismatch reduction.

stability in *c*-perpendicular growth given by the release of epitaxial strain, but not being a type of defect extrinsic to the superlattice growth.

Conclusions

In this work we have presented a structural study of high quality [$YBCO_n/PBCO_5$] superlattices with increasing YBCO layer thickness through the critical thickness for strain relaxation. Epitaxial strain due to lattice mismatch between YBCO and PBCO is significant for YBCO layers with thickness below 4 unit cells. These ultrathin layers present flat interfaces, not showing any step disorder. The relaxation of epitaxial strain in thicker layers recovers bulk lattice parameters and gives rise to rougher interfaces. Relaxation also takes place through the introduction of an inhomogeneous distribution of *c*-parallel oriented microdomains, and may play a significant role in the transport properties of such HTCS samples. Growth under such orientation provides a path for a reduction in lattice mismatch, which might favor a reduction of the interface energy in relaxed YBCO, conforming a very efficient mechanism for strain relaxation.

Acknowledgements

M. Varela was partially supported by a research grant of the Fundación Universidad Carlos III de Madrid. Financial support from CICYT grants nos. MAT94-0604 and MAT99-1706E is also acknowledged. M. Varela is thankful for the hospitality received during her stay at the NCEM-LBL. W. Grogger acknowledges support from the Max Kade Foundation for his stay at Berkeley. Work at LBNL/NCEM was supported by the Director, Office of Energy Research, Office of Basic Energy Sciences, Materials Sciences Division of the US Department of Energy under contract No. DE-AC03-76SF00098. The use of the facilities of Centro de microscopía Luis Brú is also acknowledged

References

[1] I.N. Chan, D.C. Vier, O. Nakamura, J. Hasen, J. Guimpel, S. Schultz, I.K. Schuller, Phys. Lett. A 175 (1993) 241.
[2] J.-P. Locquet, J. Perret, J. Fompeyrine, E. Mächler, J.W. Seo, G. Van Tendeloo, Nature 394 (1998) 453.
[3] M. Varela, Z. Sefrioui, D. Arias, M.A. Navacerrada, M. Lucia, M.A. Lopez de la Torre, G.D. Loos, C. Leon, F. Sanchez-Quesada, J. Santamaría, Phys. Rev. Lett. 83 (1999) 3936.
[4] M. Varela, D. Arias, Z. Sefrioui, C. León, C. Ballesteros, J. Santamaria, Phys. Rev. B 62 (2000) 12509.
[5] F. Hofer, W. Grogger, G. Kothleitner, P. Warbichler, Ultramicroscopy 67 (1997) 83.
[6] O.L. Krivanek, A.J. Gubbens, M.K. Kundmann, G.C. Carpenter, in: G.W. Bailey, C.L. Rieder (Eds.), Proc. 51st Annual Meeting Microsc. Soc. Am., San Francisco Press, San Francisco, CA, 1993, p. 586.
[7] C.L. Jia, A. Thust, G. Jakob, K. Urban, Ultramicroscopy 49 (1993) 330.
[8] F. Miletto Granozio, M. Saluzzo, U. Scotti di Uccio, I. Maggio-Aprile, Ø. Fischer, Phys. Rev. B 61 (2000) 756.
[9] C. Ballesteros, M.E. Gómez, J.I. Martín, M. Vélez, P. Prieto, J.L. Vicent, Thin Solid Films 373 (2000) 113.